HORIZON-CL6-2022-GOVERNANCE-01-07: “New technologies for acquiring in-situ observation datasets to address climate change effects”

Action acronym:	**UAWOS**
Full title:	**Unmanned Airborne Water Observing System**
Grant Agreement No:	**101081783**

UAWOS - Unmanned Airborne Water Observing System

Deliverable 3.4:
River Discharge Surveying Protocol

Date: 31 January 2025
Lead Author: Peter Bauer-Gottwein

1. Change Record

Name	Author(s)	Date	Filename
V1	Peter Bauer-Gottwein, Xinqi Hu	27 January 2025	UAWOS_D3.4 – River Discharge Surveying Protocol_v1.docx
V2	Peter Bauer-Gottwein, Xinqi Hu	28 January 2025	UAWOS_D3.4 – River Discharge Surveying Protocol_v2.docx
V3	Peter Bauer-Gottwein, Xinqi Hu, Farhad Bahmanpouri, Henrik Grosen, Daniel Wennerberg, Zhen Zhou	31 January 2025	UAWOS_D3.4 – River Discharge Surveying Protocol_v3.docx

2. Table of Contents

3. Overview and Summary

This document summarizes the contactless airborne river discharge surveying workflow developed in UAWOS. The document constitutes deliverable D3.4 of the Horizon Europe project “UAWOS – Unmanned Airborne Water Observing System”, contract number 101081783.

The UAWOS river discharge surveying workflow combines the water surface elevation surveying workflow (D3.1), the riverbed elevation surveying workflow (D3.2) and the flow velocimetry surveying workflow (D3.3). The workflow is designed to jointly estimate hydraulic roughness and river discharge through a river cross section. The basic principles of the workflow are described in Bandini et al., 2021.

The purpose of the document is to describe hardware components required for the survey, pre-survey planning procedures, field operations and post-survey data processing steps.

Moreover, the document provides an overview of typical survey productivity, expected accuracy, and spatial coverage that can be achieved in UAV river discharge surveys.

4. Purpose of the river discharge surveying workflow

River discharge is a fundamental hydrologic-hydraulic variable in water resources management, flood risk assessment and flood forecasting. It is defined as the total quantity of water in cubic meter flowing through a vertical river cross section per time.

Direct measurement of river discharge (also called river gauging) is time consuming. Classical in-situ methods for river gauging are summarized for instance in the ISO standard 748:2007 (International Organization for Standardization (ISO), 2007). Manual methods involve simultaneous measurements of flow velocity and depth at many discrete points throughout the river cross section to add up partial flow through multiple "verticals" to obtain river discharge. Generally, 20-25 verticals per river cross section are sufficient to achieve high accuracy river discharge measurements (i.e. less than 5% relative error).

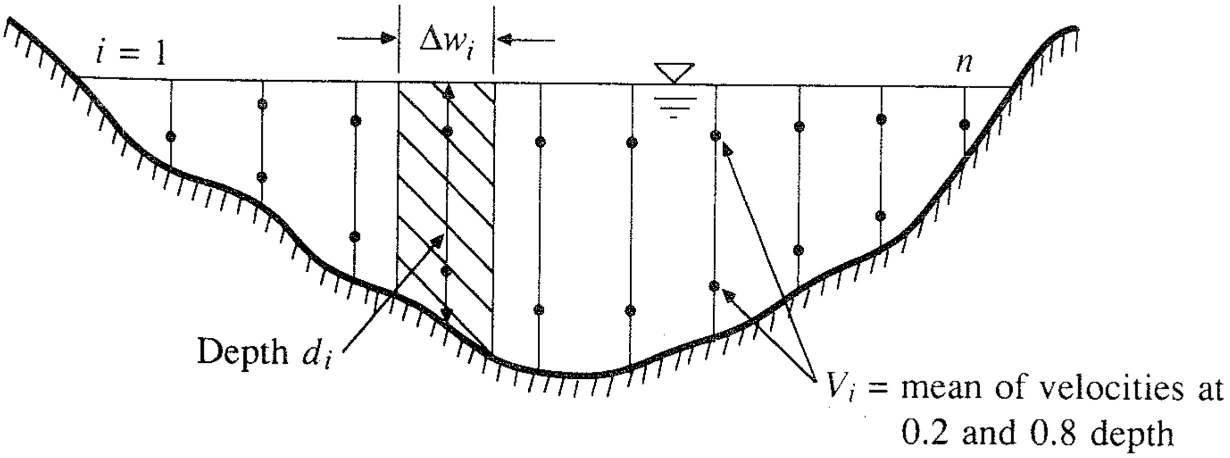

Figure 1 – "Mid-section" method of manual river gauging (reproduced from Chow, 1988)

An alternative to manual river gauging is Acoustic Doppler Current Profiling (ADCP, Gordon, 1989). ADCP has developed into the de-facto standard methodology for river discharge measurements in larger rivers. ADCP uses ultrasound signals to simultaneously measure depth and the full vertical velocity distribution in the cross section. ADCP has blind zones of a few decimeters both close to the water surface and the river bottom. In these areas, velocity must be estimated/interpolated. ADCP can be deployed from boats or remote-controlled surface vessels. However, the instrumentation must be in contact with water.

Another classical indirect in-situ method to measure river discharge is the tracer dilution method described in the ISO standard 9555-1:1994 (International Organization for Standardization (ISO), 1994). The dilution gauging method involves injecting a known quantity of a tracer at an injection site and measuring the concentration of the tracer at some distance downstream. The integral of concentration over time combined with a known quantity of tracer injected is then used to estimate the discharge, i.e. how much water is required to dilute the tracer to the observed concentration. In this method, the sensors to measure concentration must be in contact with water.

The rationale for fully contactless river discharge measurement is twofold: (1) rivers can be hard to access and dangerous. It may be time consuming and expensive to place instrumentation into the water and to fully survey the river cross section. (2) during extreme flows and floods, it is generally difficult and risky to measure flow and discharge in-situ. Also, pre-installed instrumentation may fail and/or be destroyed during extreme flows. These two arguments demonstrate the value of a contactless and airborne river discharge measurement workflow. However, contactless airborne river discharge estimates will always be less accurate than in-situ river discharge, because only surface flow velocity can be measured and not the full vertical distribution of velocity. Assumptions about the vertical velocity profile will have to be made and these assumptions may be more or less accurate in each case. Based on our experience in a range of different river environments, we expect a relative accuracy of 15% or better for contactless airborne river discharge. In general, the relative error of the contactless airborne discharge measurement decreases with increasing river size.

5. Surveying Specifications

5.1. Overall survey layout

River discharge surveys are performed for individual river cross sections (target cross section in Fig. 2). River discharge shows minor variations along the river chainage (= one-dimensional river following coordinate) in areas between tributaries. Therefore, to increase the accuracy and robustness of the river discharge estimate, several cross sections can be surveyed for the same river reach and results can be averaged (extra XS in Fig. 2).

A drone-borne river discharge survey consists of the following components (see Fig. 2):

1. Water surface elevation survey along a chainage interval of a few hundred meters around the target cross section (green in Fig. 2)
2. Riverbed elevation survey at the target cross section (brown/orange in Fig. 2)
3. River surface velocity survey at the target cross section (red in Fig. 2)

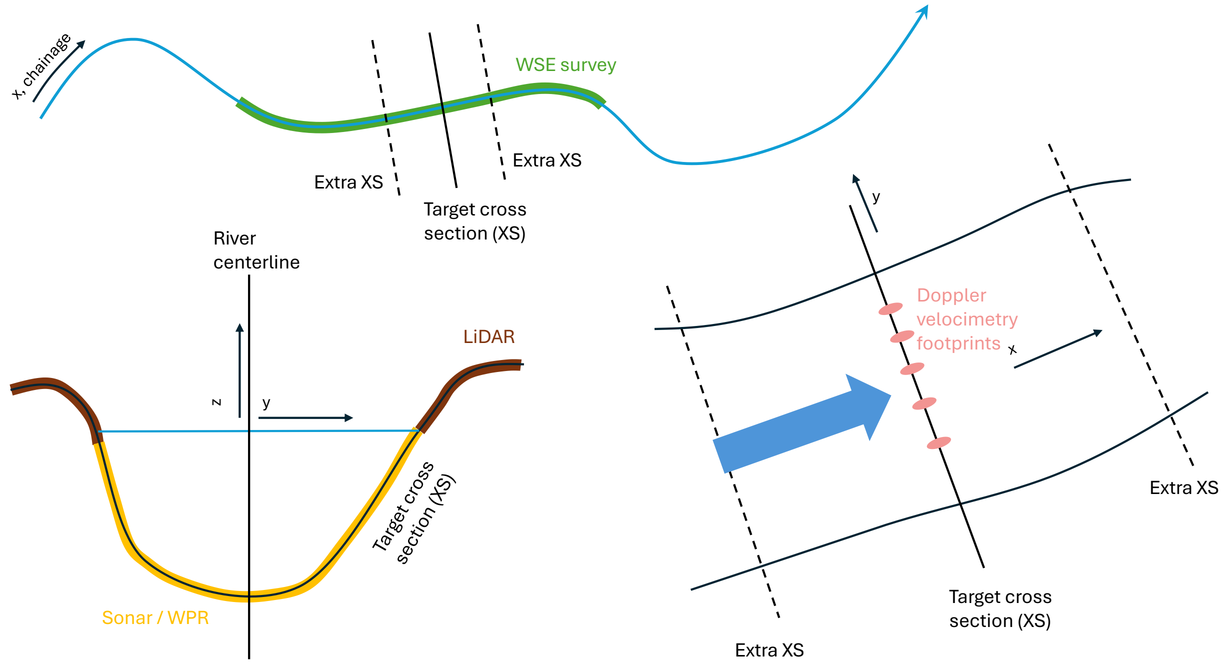

Figure 2 – Drone-borne river discharge survey layout

5.1.1. Accuracy

The expected relative accuracy is 15% or better.

5.1.2. Productivity & Scale

The productivity which can be expected is highly dependent on the survey area characteristics. Challenging accessibility to takeoff locations is a primary factor that can hamper high productivity. The actual flight time for performing a cross section is typically a few minutes. Accessibility, flight route endpoint adjustments and data verification are accountable for most of the time spent performing a river discharge cross section. Based on practical experience from a variety of rivers a productivity of 0.5-1.0 cross sections/hour can be expected.

5.2. Water surface elevation survey

The purpose of the water surface elevation (WSE) survey is to obtain the local water surface slope (WSS) at the target cross section. The WSS is the derivative of the WSE with respect to chainage and is typically given in cm/km. The water surface elevation survey should be carried out using the procedures outlined in D3.1 – WSE Surveying Protocol. The chainage interval to be surveyed around the cross section is determined by the local WSS. Generally, the surveyed interval (green in Fig. 2) should be long enough to observe a difference in WSE between the two ends of the interval of at least 10cm. For instance, if the local WSS is 50 cm/km, the length of the WSE surveying route should be at least 200 m, to allow for accurate estimation of the local WSS.

Local WSS is unknown a priori. When planning the survey, approximate expected WSS can be extracted from a digital elevation model to obtain an approximate estimate of the required length of the chainage interval to be surveyed using the WSE surveying protocol.

5.3. Riverbed elevation survey

The purpose of the riverbed elevation survey is to provide the flow cross-sectional area, i.e. the area between the water surface and the riverbed at the target cross section and any extra XS planned for the survey. The riverbed elevation survey should be carried out using the procedures outlined in D3.2 – Riverbed Geometry Surveying Protocol. Strictly speaking, only the submerged portion of the riverbed is needed for the discharge estimation. However, in most cases, apart from the discharge estimate, a rating curve at the target cross section is also desired and for this purpose, the exposed portion of the riverbed must be surveyed too (see also D4.1 – Rating Curve Estimation). Thus, a lidar survey of the exposed riverbanks is recommended, unless a high-quality (<10 cm standard error), high resolution (< 1m) DEM is available a priori.

5.4. Surface velocity survey

The purpose of the surface velocity survey is to provide the water surface velocity profile across the river at the target cross section and any extra XS planned for the survey. The surface velocity survey should be carried out using the procedures outlined in D3.3 – Flow Velocimetry Surveying Protocol.

6. Requirements and equipment

For requirements and equipment please consult D3.1 – WSE Surveying Protocol, D3.2 – Riverbed Geometry Surveying Protocol, and D3.3 – Flow Velocimetry Surveying Protocol. No additional equipment is needed for river discharge surveys and the river discharge has no additional specific requirements.

7. Post-survey Data Processing Steps

Estimation of river discharge requires the combination of water surface elevation data, riverbed elevation cross sections and river velocimetry cross sections.

7.1. Water surface elevation processing

The water surface elevation point cloud produced by D3.1 – WSE Surveying Protocol is first referenced to the river chainage, using a nearest point algorithm. Each valid WSE point is assigned the chainage of the nearest river centerline point. The result is a WSE profile along chainage as shown in Fig 3 as blue dots.

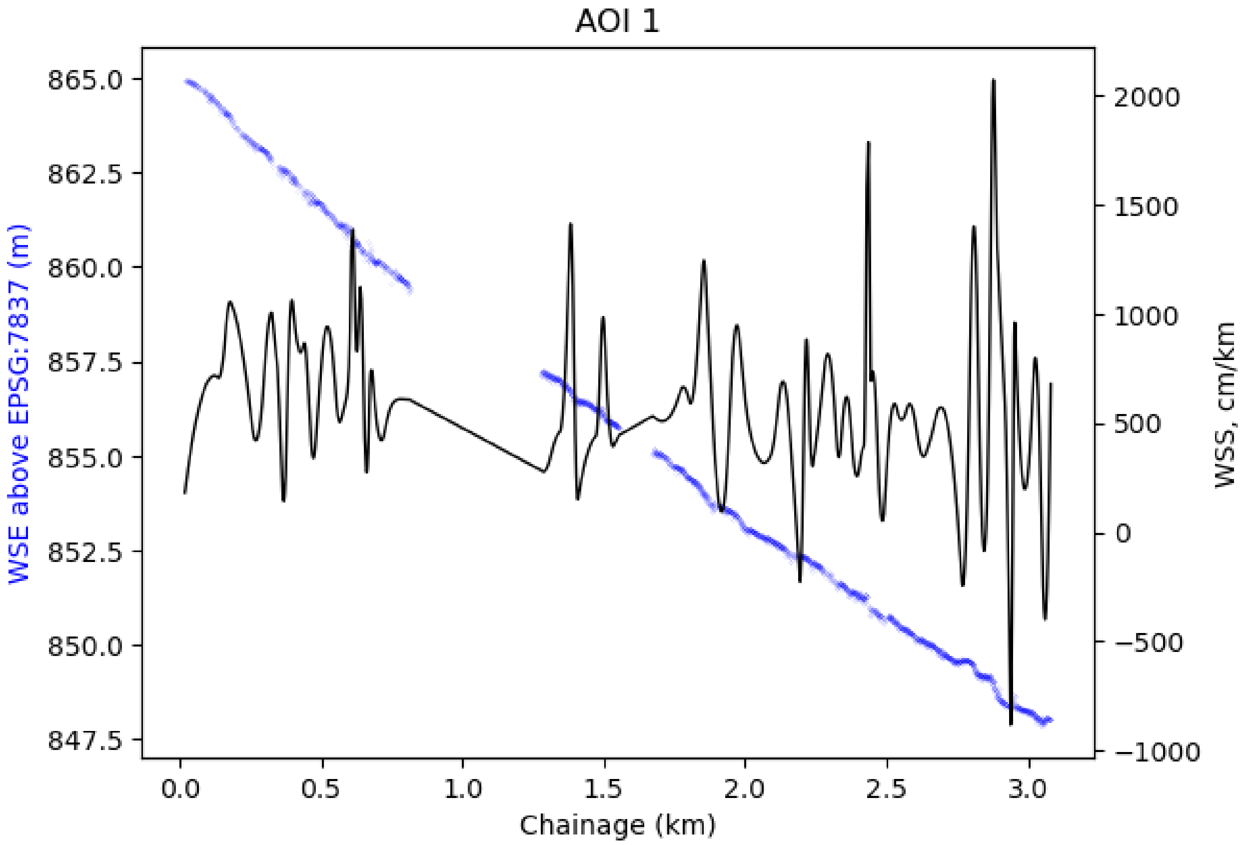

Figure 3 – Example WSE and WSS dataset from Isar River.

To derive WSS, we fit a spline interpolator with an appropriate smoothness through the point cloud. The derivative of the fitted spline can be analytically calculated and the local WSS can then be determined for every chainage point (black line in Fig 3). For the discharge calculation, we retain one local WSS estimate for each cross section of interest.

7.2. Riverbed elevation processing

Lidar and WPR/Sonar results are combined, and one river cross section geometry is produced for each cross section of interest. An example is shown in Fig 4. First, the lidar and WPR/sonar data points are reference to a common cross section reference line (aligned with the y-direction). A suitable interval on the cross-section reference line is 5 cm. Subsequently, a spline function with appropriate smoothness is fitted through the combined dataset to deliver riverbed elevation at any point along the cross section.

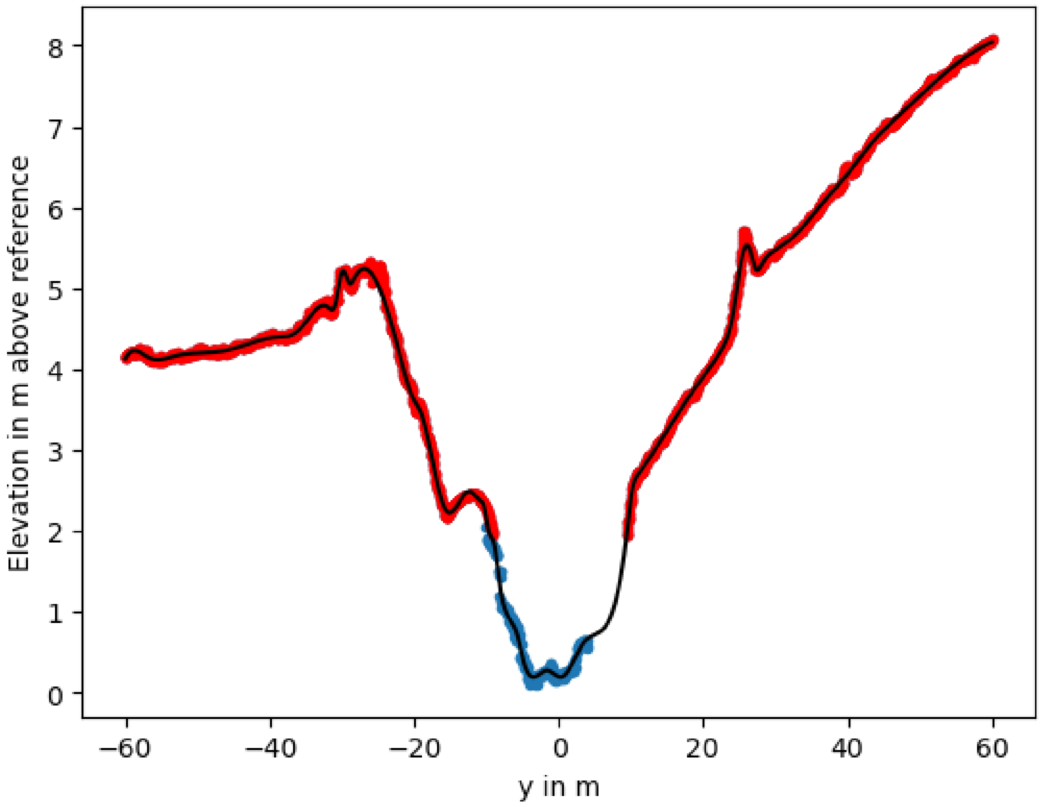

Figure 4 – Riverbed elevation processing (example data from Roenne survey). Red are lidar points, blue are WPR points. The black line is a spline interpolation through the combined dataset.

7.3. Surface velocimetry processing

Surface velocimetry points from the Doppler survey are collected. Zero velocity is assumed at the two bank coordinates and a spline function with suitable smoothness is fitted through the velocity observations to enable estimation of river surface velocity at every point along the river cross section (s. Fig 5)

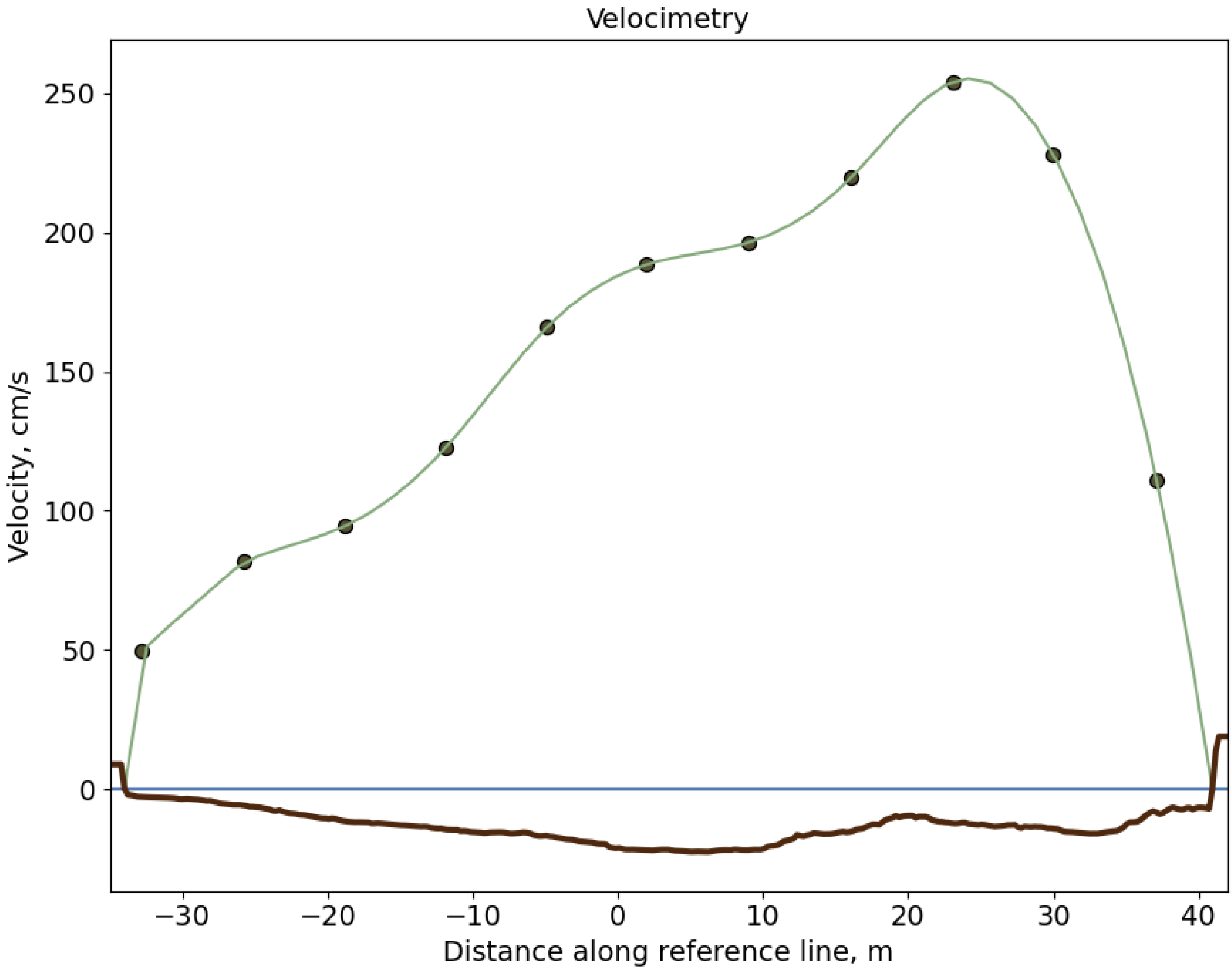

Figure 5 – Surface velocimetry processing (example from Po&Orco survey). Black dots are Doppler velocimetry, blue are water surface level, brown are bathymetry profile. The green line is a spline interpolation through the Doppler measurement.

7.4. Joint estimation of discharge and hydraulic roughness

To estimate river discharge and hydraulic roughness jointly, we combine Manning's equation, the diffusive wave approximation of the De Saint Venant equations (Chow, 1988) for open channel flow and the mid-section equation for stream gauging. Manning's equation reads

$$Q = K_s \cdot A \cdot R^{2/3} \cdot {S_f}^{1/2}$$

where Q is river discharge (m^3/s), K_s is the Strickler coefficient ($m^{1/3}/s$), A is flow cross-sectional area (m^2), R is hydraulic radius (m), i.e. flow cross sectional area divided by wetted perimeter, and S_f is friction slope, m/m.

The diffusive wave approximation of the De Saint Venant equations is equivalent to

$$S_f = WSS$$

i.e., assuming that acceleration terms in the De Saint Venant equations are negligible, we can directly observe the friction slope via the water surface slope.

The mid-section method of stream gauging reads

$$Q = \sum_{i=1}^{n} U_i \cdot d_i \cdot \Delta y_i$$

where U is the average (bulk) velocity in any vertical, and the rest of the symbols are explained in Fig. 6.

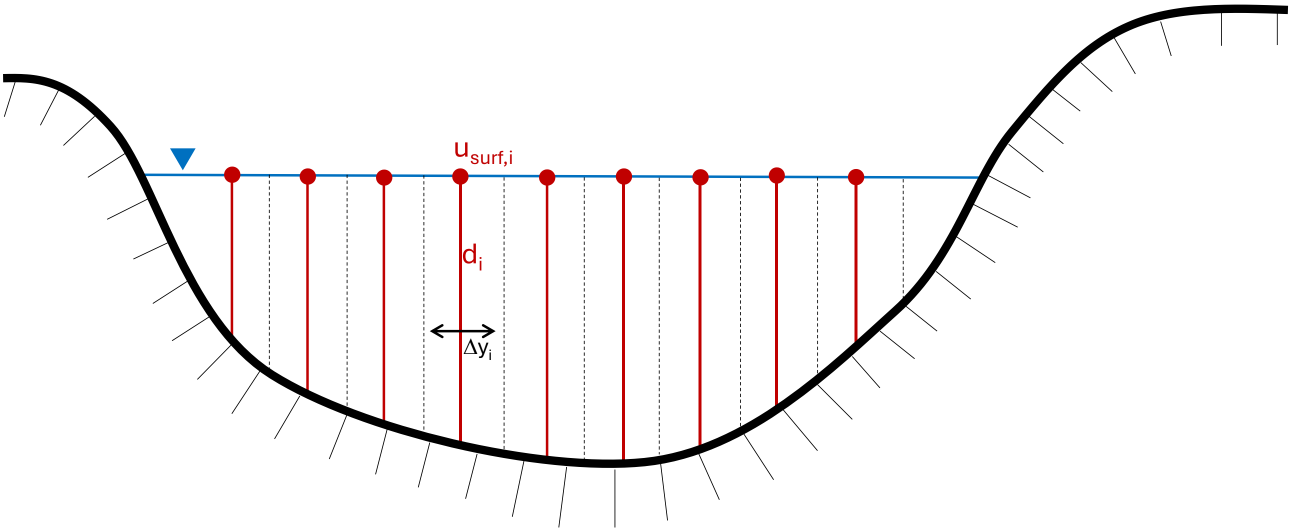

Figure 6 – Conceptual drawing illustrating the mid-section method

We can see that we have two equations with two unknowns, Q and K_S:

$$Q = K_s \cdot A \cdot R^{2/3} \cdot WSS^{1/2}$$

$$Q = \sum_{i=1}^{n} U_i \cdot d_i \cdot \Delta y_i$$

We can solve these equations iteratively and obtain estimates of the two unknowns, if we can express the bulk velocity as a function of the surface velocity and the Strickler coefficient (Bandini et al., 2021).

In order to link bulk velocity to surface velocity, we need to make assumptions about the shape of the vertical flow velocity profile. Five alternative vertical profile assumptions are available:

1. Lumped 0.85-coefficient approach
2. Logarithmic velocity profile
3. Power-law velocity profile
4. Vertical velocity profile from entropy theory
5. Vertical velocity profile from entropy theory with velocity dip

The velocity dip in river flows refers to the phenomenon where the maximum flow velocity occurs below the water surfaces. Velocity dip is mainly formed due to the existence of secondary currents and is important for narrow channels where the aspect ratio of river width/flow depth is less than 5 (Yang et al., 2004). Velocity dip causes the shift of momentum from the surface to the bottom, resulting in intensifying sediment transport.

7.4.1.Lumped 0.85-coefficient approach

Rantz, 1982 introduced a simple relationship between surface flow velocity and vertically averaged (bulk) flow velocity, the so-called 0.85 coefficient approach:

$$U = 0.85 \cdot u_{surf}$$

where u_{surf} is the surface flow velocity at each vertical obtained from the Doppler radar measurements. This approach has been used in several studies over the years and has been shown to provide robust bulk velocity estimates. Note that, in the 0.85 coefficient approach, the two equations decouple and discharge and Strickler coefficient can be calculated sequentially.

7.4.2.Logarithmic velocity profile

The standard logarithmic velocity profile (Keulegan, 1938) reads:

$$\frac{u(z)}{u_*} = \frac{1}{\kappa} \ln\left(\frac{z}{z_0}\right)$$

where κ is von Karman's constant (=0.41). Roughness length z_0 can be linked to the Strickler coefficient as (Katul et al., 2002):

$$\frac{1}{K_s} = 0.06{z_0}^{1/7}$$

For $z = d$, we have $u(d) = u_{surf}$, and then

$$u_* = \frac{\kappa \cdot u_{surf}}{\ln\left(\frac{d}{z_0}\right)}$$

Integrating the logarithmic velocity profile over the entire vertical, we derive a relationship between (observed) surface flow velocity, depth and bulk velocity:

$$U = u_{surf}\left[\frac{d}{d - z_0} - \frac{1}{\ln\left(\frac{d}{z_0}\right)}\right]$$

Note that this expression gives the bulk velocity between $z = z_0$ and $z = d$, and not between $z = 0$ and $z = d$. The logarithmic velocity profile is only used in cases where the flow depth is much larger than the roughness length, i.e. $d \approx 10 \cdot z_0$ or larger.

7.4.3.Power-law velocity profile

The standard power-law vertical velocity (Cheng, 2007) profile reads:

$$\frac{u(z)}{u_{surf}} = \left(\frac{z}{d}\right)^{1/m}$$

assuming that the maximum velocity is equal to the surface velocity and occurs at the surface. Integrating this profile over the entire vertical, we derive a relationship between (observed) surface flow velocity and bulk velocity:

$$U = u_{surf}\left[\frac{1}{\frac{1}{m} + 1}\right]$$

Following Cheng, 2007, we can link the power law exponent m to the Darcy-Weisbach friction factor:

$$m = 1.37f^{-0.43}$$

where f is the Darcy-Weisbach friction factor, which in turn can be expressed using the Strickler coefficient (Powell, 2014):

$$f = \frac{K_s^2 d^{1/3}}{g}.$$

7.4.4.Vertical velocity profile from entropy theory

Following entropy theory, we can express the vertical velocity profile as (Bahmanpouri et al., 2022):

$$u(z) = \frac{u_{surf}}{M} \ln\left(1 + (e^M - 1)\frac{z}{d}\exp\left(1 - \frac{z}{d}\right)\right)$$

where M is the entropic parameter, which can be related to Strickler's coefficient as

$$\phi(M) = \left(\frac{e^M}{e^M - 1} - \frac{1}{M}\right) = \frac{K_s d^{1/6}/\sqrt{g}}{\frac{1}{\kappa}\ln\left(\frac{d}{z_0}\right)}$$

Following entropy theory, the bulk velocity can then be calculated as

$$U = \ \phi(M) \cdot u_{surf}$$

7.4.5.Vertical velocity profile from entropy theory with velocity dip

For narrow channels (i.e. channel width over channel depth less than ca. 5), we commonly observe the phenomenon of velocity dip, i.e. the maximum flow velocity occurs not at the surface, but at some depth below the surface. The depth to the velocity maximum, called the dip, and denoted here with the symbol δ, can be estimated following Yang et al., 2004:

$$\delta = \ d\left[\frac{\alpha}{1+\alpha}\right]$$

where α is a coefficient depending on the ratio between depth and distance from the shore (s):

$$\alpha = 1.3\exp\left(-\frac{s}{h}\right)$$

The velocity dip phenomenon can be integrated into the entropy model as shown in Bahmanpouri et al., 2022. The vertical velocity distribution with velocity dip reads

$$u(z) = \frac{u_{max}}{M}\ln\left(1 + (e^M - 1)\frac{z}{d-\delta}\exp\left(1 - \frac{z}{d-\delta}\right)\right)$$

Setting $u(d) = u_{surf}$, we can find the relationship between surface velocity and maximum velocity:

$$u_{max} \ = \frac{u_{surf}}{\frac{1}{M}\ln[1 + (e^M - 1)\delta e^{1-\delta}]}$$

In situations with velocity dip, the equation for the entropic parameter becomes

$$\phi(M) = \left(\frac{e^M}{e^M - 1} - \frac{1}{M}\right) = \frac{K_s d^{1/6}\sqrt{g}}{\frac{1}{\kappa}\ln\left(\frac{d-\delta}{z_0}\right)\frac{\delta}{d-\delta}\ln\left(\frac{\delta}{d}\right)}$$

Once maximum velocity and entropic parameter are known, we get the bulk velocity from

$$U = \ \phi(M) \cdot u_{max}$$

8. Output Data Formats and Example Output

Discharge results are reported in standard csv tabular format, including cross section ID, discharge estimate and estimated uncertainty of the discharge estimate. The following table shows examples of discharge estimates compared with ground truth for various cross sections in different rivers.

Table 1. Cross section properties

XS name	XS1	XS12
XS area (m2)	763.6	706.4
Average depth (m)	1.27	1.10
Max depth (m)	2.68	2.31
Hydraulic radius (m)	1.27	1.10
Width (m)	597.8	643.3
Average surface velocity (m/s)	0.45	0.42
Max surface velocity (m/s)	0.74	0.85
Average bulk velocity from 0.85 method (m/s)	0.39	0.36
Froude number	0.13	0.13
Ground truth discharge (m^3/s)	294.6	288.1

Table 2. Discharge results

River	XS id	Method	Discharge mean (m^3/s)	Discharge std (m^3/s)	Strickler mean ($m^{1/3}/s$)	Strickler std ($m^{1/3}/s$)
Torne	XS1	0.85	281.7	1.4	34.0	0.95
		log	265.7	9.6	32.1	1.31
		power	269.7	1.5	32.6	0.14
		entropy	291.0	1.3	35.2	0.10
Torne	XS12	0.85	269.8	1.3	38.1	1.80
		log	264.1	11.8	37.2	3.66
		power	263.3	1.2	37.0	0.15
		entropy	273.5	1.3	38.6	1.29

Table 3. Error statistics

River	XS id	Method	Relative bias (%)	Relative absolute error (%)
Torne	XS1	0.85	-4.38	4.38
		log	-6.24	6.24
		power	-6.58	6.58
		entropy	-3.07	3.07
Torne	XS12	0.85	-6.35	6.35
		log	-8.34	8.34
		power	-8.63	8.63
		entropy	-5.09	5.09

9. References

Bahmanpouri, F., Eltner, A., Barbetta, S., Bertalan, L., Moramarco, T., 2022. Estimating the Average River Cross-Section Velocity by Observing Only One Surface Velocity Value and Calibrating the Entropic Parameter. Water Resour Res 58. doi:10.1029/2021WR031821

Bandini, F., Lüthi, B., Peña-Haro, S., Borst, C., Liu, J., Karagkiolidou, S., Hu, X., Lemaire, G.G., Bjerg, P.L., Bauer-Gottwein, P., 2021. A Drone-Borne Method to Jointly Estimate Discharge and Manning's Roughness of Natural Streams. Water Resour Res 57. doi:10.1029/2020WR028266

Cheng, N.-S., 2007. Power-law index for velocity profiles in open channel flows. Adv Water Resour 30, 1775–1784. doi:10.1016/j.advwatres.2007.02.001

Chow, V. Te, 1988. Applied hydrology. McGraw-Hill, New York.

Gordon, R.L., 1989. Acoustic measurement of river discharge. Journal of Hydraulic Engineering 115. doi:10.1061/(ASCE)0733-9429(1989)115:7(925)

International Organization for Standardization (ISO), 1994. ISO 9555-1:1994 Measurement of liquid in open channels - Tracer dilution methods for the measurement of steady flow.

International Organization for Standardization (ISO), 2007. Hydrometry — Measurement of liquid flow in open channels using current-meters or floats, ISO 748:2007.

Katul, G., Wiberg, P., Albertson, J., Hornberger, G., 2002. A mixing layer theory for flow resistance in shallow streams. Water Resour Res 38, 32-1-32–8. doi:https://doi.org/10.1029/2001WR000817

Keulegan, G.H., 1938. Laws of turbulent flow in open channels. J Res Natl Bur Stand (1934) 21, 707. doi:10.6028/jres.021.039

Powell, D.M., 2014. Flow resistance in gravel-bed rivers: Progress in research. Earth Sci Rev 136, 301–338. doi:10.1016/J.EARSCIREV.2014.06.001

Rantz, S.E., 1982. Measurement and computation of streamflow. doi:10.3133/wsp2175

Yang, S.-Q., Tan, S.-K., Lim, S.-Y., 2004. Velocity distribution and dip-phenomenon in smooth uniform open channel flows. Journal of Hydraulic Engineering 130, 1179–1186. doi:10.1061/(ASCE)0733-9429(2004)130:12(1179)